Simulation Sediment Transport In Development Location Of Diesel Power Plant (PLTD) Using Computational Fluid Dynamic (CFD) Methods

by Eflita Yohana

Simulation Sediment Transport In Development Location Of Diesel Power Plant (PLTD) Using Computational Fluid Dynamic (CFD) Methods

E Yohana[1], T S Utomo[1], V S Sumardi[1], D A Laksono[1], K Rozi[1], K H Choi[2]

[1] Departemet of Mechanical Engineering, Faculty of Engineering, Diponegoro University, Jl. Prof. Sudharto, SH., Tembalang-Semarang 50275, Central Java, Indonesia

[2] College of Engineering, Pukyong National University, 365 Sinseon-ro, Nam-gu, Busan 608-739, Korea

dimazaji199@gmail.com

Abstract. Research about Sediment Transport is important for the sustainability of coastal buildings. The infrastructure construction of the Halmahera Diesel Power Plant (PLTD) in the coastal area requires water supply as a cooling system. Supply of cooling water can be reduced because of erosion or sedimentation. This study uses CFD modelling of ANSYS FLUENT applications with variations in mass flow rates. Eulerian-Lagrangian approach used to predict the rate of erosion and accretion that occur around the place of Halmahera. Methods of Particle Size Distribution (PSD) numerical simulation is Uniform. Results obtained from the simulation process consist of particle mass, erosion and accretion rate in the seabed. Variations in mass flow rates of 0.05 kg / s, 0.1 kg / s, 0.15 kg / s, 0.2 kg / s, 0.25 kg / s obtained the erosion rate respectively 5.425 x 10-7 mm / year, 1,085 x 10-6 mm / year, 1,626 x 10-6 mm / year, 2,170 x 10-6 mm / year, 2,712 x 10-6 mm / year. Result of accretion rate obtained from the variation in mass flow rates is 301.43 mm / year, 602.87 mm / year, 904.30 mm / year, 1205.50 mm / year, 1507.77 mm / year.

1. Introduction

A natural process that often happens in the coastal area is a physical changed of the coastline because of coastal interaction with wave and current. This interaction will have resulted in sediment transport of coastal area (coastal sediment transport). Form of sediment transport in question is longshore sediment transport and cross-shore sediment transport. Longshore and cross-shore sediment transport will result in coastline changed. These conditions will result in accretion and erosion. Sedimentation or erosion across the coastline will have impacted the form of coastal buildings (ex: pier, jetty, wave breaker, groin, artificial sea wall, etc). By understanding the pattern of longshore and cross-shore sediment transport, than can be designed a specified construction for the intended coastal condition [1].

Halmahera, the east ternate island is a specified location for Diesel Power Plant Construction (PLTD). Diesel power plant is usually used for fulfilling the electric in low capacity, new isolated place, village, and industrial needs. Diesel power plant need a huge water consumption for its cooling system. The lack of water needs for cooling system because of sediment transport, will prevent diesel power plant to work properly [2].

This research uses the data from the temporal change of shoreline that need expensive cost and longtime research. Simulation research is needed for an efficient and effective approach. Simulation can describe spatial and temporal sediment transport because the simulation is a real conditional approach that predicts the result of analytic and calculation. The use of simulation in this research is efficient by cost and time [3].

Therefore, as a preliminary study, the model sediment transport coastal building location of the diesel power plant will use Ansys fluent software. The purpose of this modelling is to determine the rate, direction, amount of sediment transport in the construction location of Diesel Power Plant (PLTD).

2. Research Method

2.1. Validation

Validation 3D simulation is used to determine the suitable method with the realtime condition. Validation based on Tarpagkou et. al, analyzed the effect of secondary phase (solid particle) to primary phase (fluid) that happen in sedimentation tank using lagrangian DPM (Discrete Phase Mode) method. Result of the simulation that has been compared with the result of journal validation maximum 14.63% error value. Journal validation is shown in Figure 1 [4].

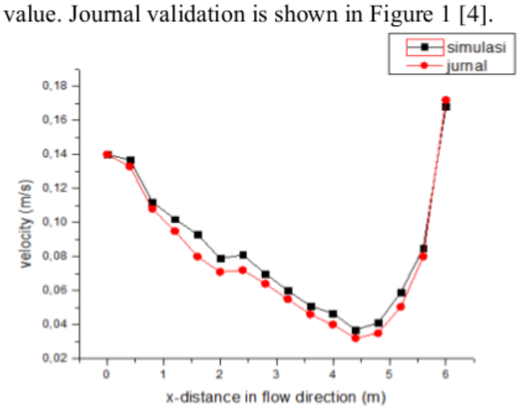

Figure 1. Journal Validation.

2.2 Modeling Area

This erosion and accretion rate modeling area is located in Halmahera, North Maluku which is geographically located at coordinates 00º41'46.6 "N - 127º32'57.7" E.

2.3 Governing Equation

The governing equation used to solve the multiphase flow between solid-liquid is the momentum, continuity and erosion-accretion equation [5]:

Continuity equation:

$$\frac{\partial \rho f}{\partial t} + \vec{V}.\left(\rho_f v_f\right) = 0 \quad (2.1)$$

Momentum equation:

$$\frac{\partial \rho_f v_f}{\partial t} + \vec{V}\left(\rho_f v_f v_f\right) = -\vec{V} + \vec{V}\,.\left[\mu\left(\vec{V}_{v_f} + \vec{V}_{v_f}^{T}\right)\right] + \rho_{fg} \quad (2.2)$$

Erosion rate and accretion equation:

$$ER = \sum_{p=1}^{N} \frac{\dot{m}_p C(d_p) f(\alpha) {v_p}^{b(v)}}{A_{face}} \tag{2.3}$$

$$R_{accretion} = \sum_{p=1}^{N} \frac{\dot{m}_p}{A_{face}} \tag{2.4}$$

The particle flow rate and velocity are represented by $\dot{m}_p$ and v_p. The term *f (a), b (v)* and $C(d_p)$ respectively shown the function of impact angle, particle relative velocity and particle diameter. A_f represents the shell face area along the wall.

2.4 Model Input Data

2.4.1. *Bathymetry.* Bathymetry map illustrates the depths of the sea and the land boundaries. The depth-sea value that has been modelled is 0-28 meters. Bathymetry map used as a reference is computational domain geometry. The boundary conditions of the computational domain model on bathymetry maps are 267x293 meters with black lines shown in Figure 2.

Figure 2. Modeling Bathymetry Map.

2.4.2 *Ocean Current*. Halmahera's ocean currents are the result of field measurements carried out in November 2017. From the results of measurements for 3x24 hours it was found that the current was dominated by non-tidal currents, where the current direction was dominated towards the north from the south-southeast direction. The current value ranges between 0-0.55 m / s with a maximum value located at a depth of 2 meters. The current data used in the simulation is north direction current with a maximum current value of 0.4 m / s [6].

2.5 Model Scenario

2.5.1. Geometry Making. Geometry Modeling was made using Solidwork based on the 267x293x28 meter bathymetry map of the waters of Halmahera. Water and sand enter from the inlet at the same speed, while the particle mass flow rate is varied. The regional boundaries (domains) taken from the research of Tarpagkou, et al. [4] can be seen in Figure 3 below.

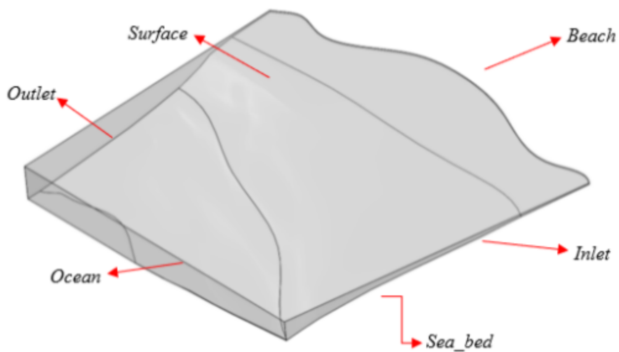

Figure 3. Computational Domain.

2.5.2. Simulation Operation Boundary Conditions. Boundary conditions used in the rate of erosion and accretion simulation refer to the results of the validation of the journal Tarpagkou, et al. Parameters for simulated boundary conditions can be seen in Table 1[7].

Table 1. Parameters of Boundary Condition Modeling of Erosion Rate and Accretion

Parameter	Value
Computational Domain	297x293x8 m
General Setting	a.Pressure-Based b.Steady
Flow Models	a.Turbulent k-epsilon Realizable b.Discrete Phase Model
Material	a.Water liquid b. Solid Particle
Boundary Conditions	a.Inlet & Ocean : Velocity Inlet b.Outlet : Outflow c.Surface : Symmetry d. Sea_bed & Pantai : Wall

2.5.3. Defining Material. The fluid used is water, while the solid phase uses sand particles with properties as shown in Table 2.

Table 2. Material properties

Material properties	Value	Unit
Sea water density	1025	kg/m^3
Density of sand particles	2650	kg/m^3
Water viscosity	0,001003	Ns/m^2
Particle diameter	0,05	mm
Velocity	0,4	m/s

3. Result and Discussion

3.1. Contour of Sediment Concentration

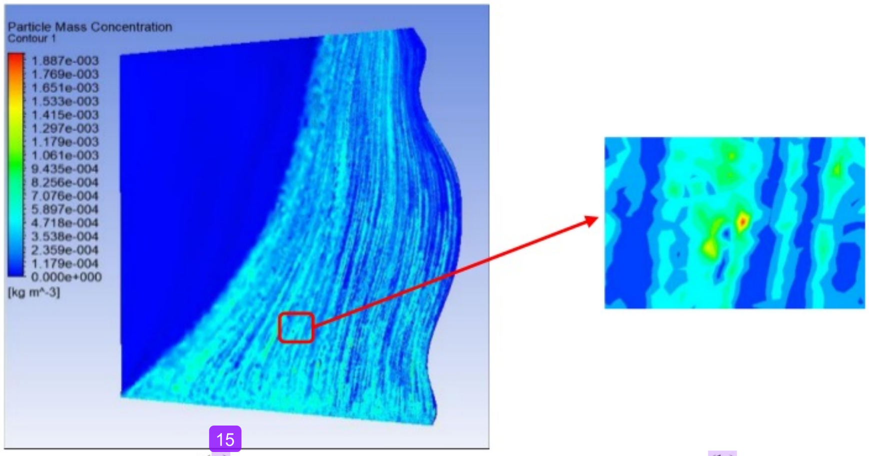

(a) (b)

Figure 4. (a) Contour of particle mass concentration. (b) Enlargement of the highest value of particle mass concentration.

Figure 4 shows the particle mass concentration contour explains the pattern of sediment distribution in Halmahera waters, which is dominated towards the north according to the data from the analysis condition of Halmahera waters in 2017. The sediment concentration in the area around the inlet is higher compared to the surrounding area outlet. This is because the particle velocity in the vicinity of the inlet is slowers than the particle velocity in the outlet as in the study of Ido, et al. [8].

3.2 Erosion and Accretion Rate Contours

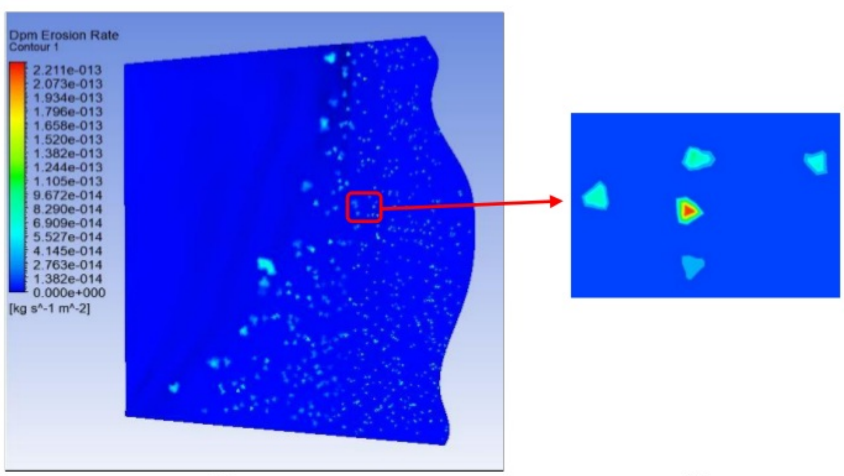

(a) (b)

Figure 5. (a) Contour of erosion rate. (b) Enlargement of the highest erosion rate.

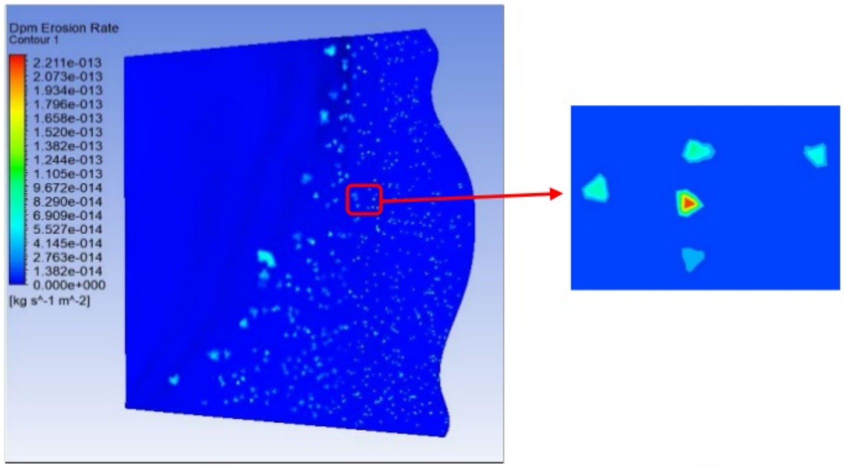

(a) (b)

Figure 6. (a) Accretion contour. (b) Enlargement of the highest value of accretion rate

In Figure 5 and Figure 6 the direction of the spread of erosion rate and accretion rate can be seen. In this simulation the variation of particle mass flow rate is 0,05 kg/s, 0,1 kg/s, 0,15 kg/s, 0,2 kg/s, and 0,25 kg/s with input speed equal 0,4 m/s. The particle mass flow rate is the number of particles that can be moved in one second. The more particles injected, the higher concentration of particles in the water flow which makes the frequency of particles collide with the wall of the seabed increases. The worst erosion and accretion occurred when the particle mass flow rate was the highest value of 0,25 kg/s. The Fluent simulation shows the same contour on each particle variable, in the form of erosion and accretion points due to the collision of sand particles after crossing the sea_bed wall.

3.3 *Conversion of Erosion and Accretion Rate Units*

Based on the results of the simulation of the rate of erosion and accretion with variations in particle mass flow rates obtained. The unit results of the simulation of the rate of erosion and accretion are kg/m^2.s, this value will be converted into units of mm/year to predict the rate of erosion and accretion that occurs around Halmahera waters within one year [9].

$$ER\,/\,R_{accretion}\left(\frac{mm}{tahun}\right)=\frac{ER\left(\frac{kg}{m^2s}\right)}{\rho\left(\frac{kg}{m^3}\right)}\;x\;1000\left(\frac{mm}{m}\right)\;x\;3600\left(\frac{s}{hr}\right)\;x\;24\left(\frac{hr}{day}\right)\;x\;365\left(\frac{day}{year}\right)$$

The results of the conversion of erosion rate units and maximum accretion based on variations in particle mass flow rates can be seen in Table 3.

Table 3. Results of simulation of erosion and accretion rates

Particle mass flow rate	Maximum erosion rate		Maximum accretion rate	
kg/s	kg/m^2.s	mm/year	kg/m^2.s	mm/year
0,05	4,559 x 10^{-14}	5,425 x 10^{-7}	2,533 x 10^{-5}	301,43
0,1	9,119 x 10^{-14}	1,085 x 10^{-6}	5,066 x 10^{-5}	602,87
0,15	1,367 x 10^{-13}	1,626 x 10^{-6}	7,599 x 10^{-5}	904,30
0,2	1,824 x 10^{-13}	2,170 x 10^{-6}	1,013 x 10^{-4}	1205,50
0,25	2,279 x 10^{-13}	2,712 x 10^{-6}	1,267 x 10^{-4}	1507,77

Conversion results are then plotted into a graph between the maximum erosion and accretion rate values with variations in particle mass flow rates. The graph of the variation in particle mass flow rate with maximum erosion and accretion rate can be seen in Figure 7.

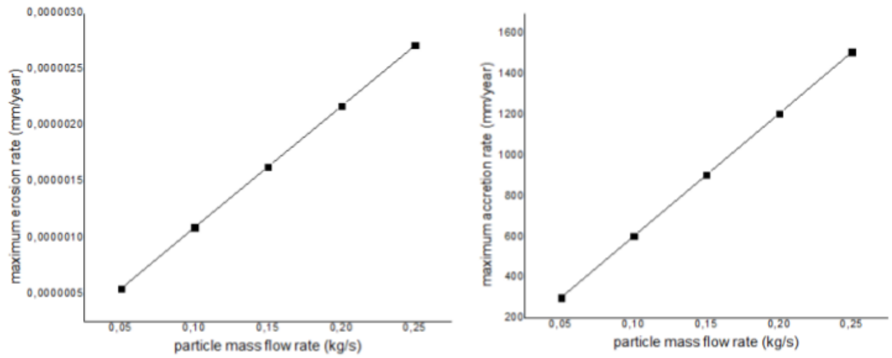

(a) (b)

Figure 7. (a) The graph of the relationship between particle mass flow rate and erosion rate. (b) The graph of the relationship between the mass flow rate of a particle to the rate of accretion.

Figure 7 illustrates the relationship between the particle mass flow rate with the rate of erosion and accretion is directly proportional. It can be concluded that the higher the particle mass flow rate, the greater the rate of erosion and accretion. Increased particle mass flow affects the rate of erosion and accretion to increase. It can be seen that the rate of erosion and accretion in the graph where the highest particle mass flow rate of 0.25 kg/s results in the highest rate of erosion and accretion.

When the particle mass flow rate is high enough, the particle mass flow rate will approach the velocity of the fluid. The worst erosion and accretion occurred when the particle mass flow rate was of the highest value of 0.25 kg/s. A small increase in the particle mass flow rate can result in a considerable increase in the rate of erosion and accretion [10]. The graph in Figure 7 has the same graph trend as Hariri Dwi Kusuma's research as shown in Figure 8.

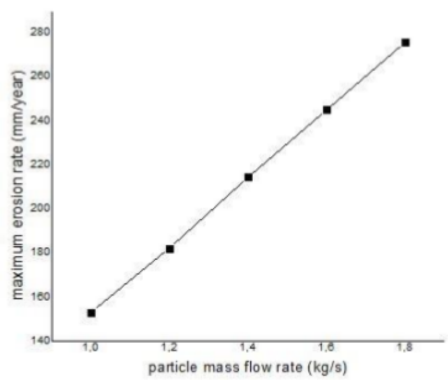

Figure 8. Graph of the relationship between particle mass flow rate to maximum erosion rate in previous research (Kusuma, 2014).

4. Conclusion

The model of sediment distribution pattern in Halmahera waters is predominantly headed north in accordance with the data from the analysis of the condition of Halmahera waters in 2017. Sediment concentrations in the area around the inlet are higher than the area around the outlet. With different particle mass flow rates of 0,05 kg/s, 0,1 kg/s, 0,15 kg/s, 0,2 kg/s, 0,25 kg/s obtained an erosion rate of $5{,}425 \times 10^{-7}$ mm/year, $1{,}085 \times 10^{-6}$ mm/year, $1{,}626 \times 10^{-6}$ mm/year, $2{,}170 \times 10^{-6}$ mm/year, $2{,}712 \times 10^{-6}$ mm/year. From the variation of the particle mass flow rate, the accretion rate obtained are 301,43 mm/year, 602,87 mm/year, 904,30 mm/year, 1205,50 mm/year, 1507,77 mm/year. By the data increasing the particle mass flow rate has an effect on increasing the rate of erosion and accretion.

Nomenclature

d_p	Particle diameter (m)	A	Surface area (m^2)
m_p	Particle mass flow rate (kg/s)	ER	Erosion rate ($kg/m^2.s$)
v	Velocity (m/s)	$R_{accretion}$	Accretion rate ($kg/m^2.s$)
V_r	Particle relative velocity (m/s)	g	Gravity (m/s^2)
ρ_f	Fluid density (kg/m^3)	α	Collision angle (°)
ρ_p	Density of particle (kg/m^3)	μ	Viscosity (Ns/m^2)

References

[1] Istiyanto D Catur 1989 *Overview of Methods for Longshore Sediment Transport Countries* (Yogyakarta: Gadjah Mada University Civil Engineering Departement)

[2] Susiati H and Mellawati J 2013 Mapping of the Substrate Base Substrate Distribution of Coastal Water on the Muria Peninsula in Jepara Regency *Journal of Nuclear Energy Development* **15** 1 pp 55-62

[3] Latief H 2002 *Oceanography Beach* (Bandung: Bandung Institute of Technology)

[4] Tarpagkou R and Pantokratoras A 2013 CFD Methodology for Sedimentation Tanks: The Effect of Secondary Phase on Fluid Phase Using DPM Coupled Calculations *Appl. Math. Model* **37** 5 pp 3478–94

[5] Kannojiya V, Darshan M B, and Chandra Y P 2018 Numerical Analysis of Erosion Wear and Drop Pressure for Turbulent Multiphase Slurry Flow of Bottom Ash-Water in Slurry Pipe, *Arch. Mech. Eng.* **65** 3 pp 361-78

[6] Results of Analysis of Halmahera Water Conditions 2017

[7] ANSYS 2017 *ANSYS Fluent Theory Guide* (Pennsylvania: SAS IP Inc.)

[8] Yudhatama I W, Hidayat M I P, and Jatimurti W 2018 Simulation of Computational Fluid Dynamics (CFD) Erosion of Sand Particles in Turbulent Gas Fluid Flow in Vertical-Horizontal Pipe Elbows *J. Tek. ITS* **7** 2 B134-9

[9] Mohyaldinn M, Noaman E, and Ismail M 2011 *Evaluation of Different Modeling Methods Used for Erosion Prediction* (Malaysia: Universiti Teknologi Petronas Mechanical Engineering Department)

[10] Kusuma H D and Utomo T S 2014 Analysis of the Effect of Solid Particle Flow Rate on Turbine Blades of Reaction in Steam Power Generation Systems Using CFD *J. Rotasi* **2** 4 pp 488-95

Simulation Sediment Transport In Development Location Of Diesel Power Plant (PLTD) Using Computational Fluid Dynamic (CFD) Methods

ORIGINALITY REPORT

10%	7%	8%	%
SIMILARITY INDEX	INTERNET SOURCES	PUBLICATIONS	STUDENT PAPERS

PRIMARY SOURCES

1	www.ibpsa.org Internet Source	1%
2	www.gnest.org Internet Source	1%
3	Mirhadi Zeynalian, Amir Hossein Hajialirezaei, Amir Reza Razmi, M. Torabi. "Carbon Dioxide Capture from Compressed Air Energy Storage System", Applied Thermal Engineering, 2020 Publication	1%
4	link.springer.com Internet Source	1%
5	Sukmanto Dibyo, Ign. Djoko Irianto, V. I. Sri Wardani, Marliyadi Pancoko. "ANALYSIS ON FLOW PRESSURE IN THE PNEUMATIC BRAKING SYSTEM OF FHS-RDE USING FLUENT 6.3 SOFTWARE", JURNAL TEKNOLOGI REAKTOR NUKLIR TRI DASA MEGA, 2020	1%

Publication

6	www.nahje.com Internet Source	<1 %
7	onepetro.org Internet Source	<1 %
8	curve.coventry.ac.uk Internet Source	<1 %
9	Paulo N. Baptista, Fernanda A.R. Oliveira, Jorge C. Oliveira, Sudhir K. Sastry. "Dimensionless analysis of the flow of spherical particles in two-phase flow in straight tubes", Journal of Food Engineering, 1997 Publication	<1 %
10	studentsrepo.um.edu.my Internet Source	<1 %
11	Jerzy Merkisz, Jacek Pielecha. "Nanoparticle Emissions From Combustion Engines", Springer Science and Business Media LLC, 2015 Publication	<1 %
12	manualzz.com Internet Source	<1 %
13	ntrs.nasa.gov Internet Source	<1 %
14	Somchai Wongwises, Paisarn Naphon. "Heat Transfer Characteristics of a Spirally Coiled,	<1 %

Finned-Tube Heat Exchanger under Dry-Surface Conditions", Heat Transfer Engineering, 2006
Publication

---

15 José Antonio Soriano, Reyes García-Contreras, David Leiva-Candia, Felipe Soto. "Influence on performance and emissions of an automotive diesel engine fueled with biodiesel and paraffinic fuels: GTL and bio-jet fuel Farnesane", Energy & Fuels, 2018 <1%
Publication

---

16 repository.up.ac.za <1%
Internet Source

---

17 energiatehokkaasti.fi <1%
Internet Source

---

18 C. K. Shum, Chung-Yen Kuo. "Chapter 7 Observation and Geophysical Causes of Present-Day Sea-Level Rise", Springer Science and Business Media LLC, 2010 <1%
Publication

---

19 HU LI, YUJI TOMITA. "A NUMERICAL SIMULATION OF SWIRLING FLOW PNEUMATIC CONVEYING IN A HORIZONTAL PIPELINE", Particulate Science and Technology, 2000 <1%
Publication

Tat Leung Chan, Shuyuan Liu, Yan Yue.

20	"Nanoparticle formation and growth in turbulent flows using the bimodal TEMOM", Powder Technology, 2018 Publication	<1%
21	J.R. Miles, P.E. Russell, B.G. Ruessink, D.A. Huntley. "Field observations of the effect of shear waves on sediment suspension and transport", Continental Shelf Research, 2002 Publication	<1%

Exclude quotes	Off	Exclude matches	Off
Exclude bibliography	Off		

Simulation Sediment Transport In Development Location Of Diesel Power Plant (PLTD) Using Computational Fluid Dynamic (CFD) Methods

GRADEMARK REPORT

FINAL GRADE

/0

GENERAL COMMENTS

Instructor

PAGE 1

PAGE 2

PAGE 3

PAGE 4

PAGE 5

PAGE 6

PAGE 7

PAGE 8